

Apical localization of glutamate in GLAST-1, glutamine synthetase positive ciliary body nonpigmented epithelial cells

Marlyn P Langford¹
 Jeffrey M Gosslee¹
 Chanping Liang¹
 Dequan Chen¹
 Thomas B. Redens¹
 Tomas C Welbourne²

¹Department of Ophthalmology,

²Department of Cellular and Molecular Physiology, Louisiana State University Health Sciences Center, Shreveport, LA, USA

Abstract: The distribution of glutamate (Glu), the Glu transporter GLAST-1, and glutamine synthetase (GS) in human and monkey anterior uveal tissue, as well as serum (S) to aqueous humor (AH) Glu and glutamine (Gln) gradients were investigated. Cross-linked Glu (xGlu), GLAST-1, and GS were detected using the immunofluorescent antibody technique. S/AH Glu, Gln, and alanine (Ala) concentrations were quantified by high performance liquid chromatography. xGlu immunoreactivity was detected in melanocytes, posterior pigmented epithelial/dilator muscle cells, vascular endothelial cells, and lymphocytes of the iris, as well as the pigmented (PE) and nonpigmented epithelial (NPE) cells and muscle cells of ciliary body. xGlu immunoreactivity was highly concentrated at the apices of GLAST-1, GS positive ciliary body NPE cells, and in GLAST-1 positive iris melanocytes and iris dilator muscle cells. AH Glu concentrations were lower ($p < 0.001$), while Gln was higher in monkey ($p = 0.01$) and human cataractous ($p = 0.15$) AH than serum. The results indicate that Glu is concentrated within GLAST-1, GS positive NPE cells and are consistent with the suggestion that Glu and Gln concentrations in AH may be due in part to GLAST-1 and GS activity in iris and ciliary body epithelial cells.

Keywords: ciliary body, eye, glutamate, glutamine synthetase, nonpigmented epithelial cells, uvea

Introduction

Cells within ocular tissue, as well as other tissues of the body, take up and utilize Glu for energy, protein, and nucleic acid synthesis. The cellular distribution of Glu, as well as several other amino acids, has been extensively mapped in zebrafish iris, ciliary body, and retinal tissues (Marc and Cameron 2001) and in primate and feline retinal tissue (Kalloniatis et al 1996; Marc et al 1998). Notably, some cells contain high concentrations of Glu (Ehinger 1977; Davanger et al 1991; Kalloniatis et al 1996; Marc and Cameron 2001). Moreover, uptake and metabolism of Glu by retinal cells is essential for normal retinal function. Accordingly, the uptake of extracellular Glu by the high affinity Na^+/K^+ -dependent excitatory amino acid transporters (EAAT) (for review see Arriza 1994; Kanai et al 1994; Schultz and Stell, 1996; Lehre et al 1997; Arriza et al 1997; Lim et al 2005) is critical to glutamatergic function, preventing the neurotoxicity caused by over-stimulation of the Glu receptor by elevated extracellular Glu levels (Choi et al 1987) and regulating gap junction communication between glia and astrocytes (Enkvist and McCarthy 1994). Further, it has been suggested that the rapid uptake of Glu by GLAST-1 (EAAT-1) and conversion to Gln by GS (converts Glu plus ammonia to Gln) in retinal Müller cells (Riepe and Norenberg 1978; Rauen et al 1998; Shen et al 2004) protects against Glu neurotoxicity, inhibits ammonia neurotoxicity (Derouiche and Rauen 1995; Shaked et al 2002), and regulates glial cell swelling (Izumi et al 2004). Notably, GS is the only intracellular enzyme that can convert Glu to Gln and is highly concentrated in organs that appear to function

Correspondence: Marlyn P Langford
 Department of Ophthalmology, LSU
 Health Sciences Center, 1501 Kings Hwy/
 PO Box 33932, Shreveport,
 LA 71130-3932, USA
 Tel +1 318 675 5010
 Fax +1 318 675 6000
 Email mlangf@lsuhsc.edu

primarily to remove Glu or ammonia (van Staaten et al 2006). Concomitantly, the accumulation of Glu in retina and lens (Reddy 1967) and the lower than plasma concentrations (≤ 20 μM) of Glu in AH and vitreous humor of most mammals (Reddy 1967; Reddy et al 1977; Wu et al 1988; Dreyer et al 1996; Wamsley et al 2005) suggest Glu is actively removed from the AH and vitreous.

The distribution of acidic amino acid transporters (ie, EAATs) in anterior uveal tissues, especially the PE and NPE cells of the ciliary body and posterior iris, is unknown. However, it is well known that Glu and other amino acids are actively transported across the ciliary body into the AH (Reddy 1967; Reddy et al 1977) and are taken up and utilized by the lens (Jernigan and Zigler 1987; Jernigan 1990; Lim et al 2005). The results of previous studies have demonstrated EAAT expression in rabbit ciliary body tissue and have suggested that inhibition of the Glu transport elevates AH Glu levels and increases paracellular permeability of the blood – aqueous barrier (BAB) epithelium (ie, passage of serum protein between ciliary body epithelial cells) (Langford et al 1997; 1999). The modulatory effect of Glu on the paracellular permeability pathway is also supported by *in vitro* studies showing that inhibition of extracellular Glu generation or high-affinity Glu transport decreases the accumulation of Glu (Meade et al 1998) and increases epithelial cell monolayer paracellular permeability (Welbourne et al 1996).

The following immunohistological studies were performed to determine the distribution of xGlu immunoreactivity in human and monkey iris and ciliary body tissues. In addition, the co-localization of GLAST-1 (EAAT-1) and GS with xGlu immunoreactivity was determined in human ciliary body tissues. Lastly, the serum to AH concentration gradients for Glu and Gln, as well as alanine (Ala), in humans and monkeys were assessed. The results show xGlu and GLAST-1 immunoreactivity in epithelial, endothelial, and muscle cells of iris and ciliary body tissue. Notably, high concentrations of xGlu immunoreactivity were detected at the apical surface of GLAST-1 and GS positive ciliary body NPE cells. Concomitantly, the concentration of Glu was lower while the Gln concentration was higher in AH than serum.

Materials and methods

Tissue samples

Three nondiabetic, phakic human cadaver eyes were obtained on ice from the Northwest Louisiana Eye Bank (Shreveport, LA) and processed for histological analysis upon arrival

(Table 1). A venous blood sample (0.2–2.5 ml) and an AH sample (25–85 μl from the anterior chamber) was collected from 18 consenting adults during intraoperative cataract surgery. The experimental protocols were approved by the LSU Health Sciences Center Internal Review Board for the Protection of Human Research Subjects and were performed in accordance with the tenets of the Declaration of Helsinki.

AH and venous blood samples were collected from 5 adult rhesus monkeys within 15 minutes of euthanasia (*Macaca mulatto*; Dr Louis N. Martin, Tulane Regional Primate Research Center, Tulane University Medical Center, Covington, LA) and placed on ice. One eye from two monkeys was excised within 30 min of death and processed for histological analysis as per human eyes. AH and blood samples were centrifuged (5,000Xg for 3 min) to remove cellular components and the AH and serum processed for amino acids quantification or stored at -100 °C. The experimental protocols were approved by the LSU Health Sciences Center and Tulane Regional Primate Research Center Animal Care and Resources Committees and were performed according to NIH statement for the Care and Use of Laboratory Animals in Research.

Histological sections

Two 0.5X1.0 cm bands composed of cornea rim (1–2 mm) and sclera with attached iris, ciliary body, and retina were removed quickly from 3 human cadaver and 2 monkey eyes. The excised tissue was gently rinsed in cold phosphate buffered saline (PBS) and fixed for 30 min in cold 0.4% paraformaldehyde, placed in Tissue Tek[®] O.C.T. embedding media (Miles, Inc., Elkhart, IN) and frozen (-100 °C). Serial cryostat sections were cut, placed on glass slides, and air-dried as previously reported (Langford et al 2006). Slides were stored dry at -20 °C until used.

Immunoreagents

Rabbit antibodies raised to cross-linked Glu (anti-xGlu) were purchased from Chemicon International (Temecula, CA; www.chemicon.com) and Signature Immunologics (Chromatag E30-Red; www.immunologics.com). Polyclonal goat anti-GS antibody (ab6585) was purchased from Abcam, Inc. (Cambridge, MA). Guinea pig polyclonal antibody to C-terminal peptide of rat GLAST-1 was purchased from Chemicon. Secondary antibodies used included TRITC-tagged goat anti-rabbit immunoglobulin G (IgG) (absorbed with human IgG) (Sigma, St Louis, MO), FITC-conjugated goat anti-rabbit IgG (Fab') (Cappel; Organon Teknika Corp.,

Table 1 Age, sex, cause of death, and past medical history for three nondiabetic, phakic human cadaver eyes

Eyes	Age	Sex	Cause of death	Past medical history	PMD ^a
1 (OS)	82	F	Cardiopulmonary arrest	Parkinson's disease	2
2 (OD)	78	F	Cardiac arrest	None	5
3 (OS)	74	M	Cardiac arrest	None	5

Note: ^aPMD, Postmortem delay; hours between the time of death and time of procurement and processing.

West Chester, PA), FITC-labeled rabbit anti-goat IgG (Cappel) and FITC-tagged goat anti-guinea pig IgG (Sigma). Horse-radish peroxidase (HRP)-linked anti-guinea pig and anti-goat IgGs were purchased from Jackson ImmunoResearch Laboratories (West Grove, PA).

Immunofluorescent antibody assay

The immunofluorescent antibody (IFA) assay using polyclonal antibodies to xGlu, GLAST-1, and GS was performed as previously described (Chen et al 2005; Langford et al 2006). Briefly, double labeling studies for anti-xGlu immunoreactivity with GLAST-1 or GS were performed on duplicate uveal tissue sections from 3 human and 2 monkeys on three slides each. Sections were covered with 0.1 ml of PBS containing of 1:40 dilution of E30 Red-tagged rabbit anti-xGlu antibody (ie, direct IFA) or with 0.1 ml PBS containing onto 1:1,000 dilution of rabbit anti-xGlu polyclonal antibody (ie, for indirect IFA) and incubated in humidified atmosphere overnight at 37 °C. Unreacted primary antibodies to xGlu were removed by 6 rinses of PBS. Secondary antibody (1:1,000 dilution of TRITC-tagged goat antibody to rabbit IgG in PBS) was pipetted onto sections reacted with rabbit anti-xGlu antibody and incubated in a humidified atmosphere for 6 h at 37 °C. Unreacted secondary antibodies were removed by 6 rinses with PBS. For dual GLAST-1 and xGlu immunoreactivity IFA, a 1:100 dilution of guinea pig anti-GLAST-1 antibody was pipetted onto sections previously reacted with rabbit anti-xGlu antibody and TRITC-tagged goat anti-rabbit IgG secondary antibody. After incubation overnight at 4 °C, a 1:1,000 dilution of FITC-tagged rabbit anti-guinea pig IgG was pipetted onto sections and incubated in humidified atmosphere at 37 °C for 6 h. For dual GS and xGlu immunofluorescent IFA, a 1:1,000 dilution of goat anti-GS antibody was applied to the sections previously reacted with E30 Red-tagged rabbit anti-xGlu antibody. After overnight incubation at 4 °C, unbound anti-GS antibody was removed by 6 rinses of PBS. One-tenth ml of a 1:1,000 dilution of FITC-tagged rabbit anti-goat IgG was pipetted onto each section and incubated for 6 h at 37 °C. Concomitantly, control sections were incubated in PBS containing

1:1,000 dilutions of goat or rabbit serum, rinsed 6 times, and reacted with TRITC and FITC-conjugated secondary antibodies. All slides were rinsed 6 times with PBS to remove unreacted secondary antibody. Excess PBS was blotted from the slides, cover slips were applied with IFA mounting media (Calbiochem), and all slides were stored in the dark at 4 °C. Immunofluorescence was observed using a 40x .60 N.A. plan fluor objective on a Nikon Eclipse TE300 inverted microscope with an epi-fluorescence attachment, using a Chroma 83000 filter set with single band excitors for FITC (492nm/18x) or TRITC and R30 Red (572nm/23x) in the filter wheel and a stationary multi-band beam splitter and emission filter. Images were captured with a Photometrics Cool SNAPfx monochrome CCD camera controlled with Scanalytics IPLab software.

Western immunoblot analysis

Iris, ciliary body, and retinal layers (temporal, central, mid-third) were micro-dissected from the cadaver eyes under a 10X binocular microscope. Iris, ciliary body (CB), retinal pigment epithelial (RPE), and retinal nerve fiber layer (NFL) tissue (10 mg) was placed in 0.3 ml of lysis buffer (50 mM HEPES, 10 mM CHAPS [3-[(3-cholamidopropyl) dimethylammonium]-1-propanesulfonic acid], 5 mM dithiothreitol, pH 7.4). The tissues were frozen, thawed, and centrifuged at 15,000Xg at 4 °C for 10 min. The supernatant fluids were recovered into labeled vials, the protein concentrations were determined (BioRad Protein Assay) and each was diluted to 1 mg/ml in lysis buffer containing 1mM PMSF (phenylmethylsulfonyl fluoride; Sigma). The proteins in each sample (5 µ/20 µl Laemmli sample buffer; BioRad) were separated by 1% sodium dodecylsulfate –10% polyacrylamide gel electrophoresis (PAGE) in Tris/Glycine/SDS running buffer (BioRad), and transblotted onto a Hybond-P polyvinylidene difluoride membrane (Fischer Scientific). After overnight incubation with a 1:1,000 dilution of goat antibody to GS or 1:100 dilution of guinea pig anti-GLAST-1 antibody, the immunoreactive protein bands were visualized utilizing HRP-linked anti-guinea pig IgG or anti-goat IgG as previously described (Chen et al 2005). Protein standards were

included in one lane of each gel run (Precision Plus Protein™ Dual Color Standard, BioRad).

Amino acid quantification

Fifty microliters of each clarified (ie, centrifuged at 5,000Xg for 5 min) AH and serum sample were immediately placed in 50 µl of 10% trichloroacetic acid (to inhibit the conversion of Gln and Glu prior to analysis) (Fonseca-Wollheim 1990). Samples were stored at -100 °C until the concentrations of Glu, Gln, and Ala were quantified by high performance liquid chromatography as previously described (Langford et al 1997).

Results

Detection of xGlu immunoreactivity in human anterior uveal tissues by IFA

Anterior uveal tissue sections from 3 human cadaver eyes (Table 1) were reacted with anti-xGlu antibody and the xGlu immunoreactivity visualized in cells by IFA analysis (Figure 1). XGlu immunoreactivity was detected in anterior iris melanocytes, pigment containing epithelial cells/dilator muscle cells along the posterior iris surface, PE cells, and NPE cells of the anterior corona ciliaris (*pars plicata*) of all human ciliary body sections (Figure 1A, B). In addition, xGlu immunoreactivity was detected in iris and the ciliary body blood vessels, lymphoid cells, and human ciliary muscle. High concentrations of xGlu immunoreactivity were localized to PE and NPE cells (Figure 1 C–F). Notably, xGlu immunoreactivity was concentrated at the apical surfaces of NPE cells and was juxtaposed to the apically localized pigment granules in the PE cells (Figure 1E, F). The possibility that disease, post mortem changes, and melanin pigment may affect the distribution of the xGlu signal within a tissue or cell cannot be discounted. In contrast, very weak immunofluorescent staining for immunoreactive xGlu was detected in the interstitial tissue between the capillary blood vessels and the ciliary epithelial cells (Figure 1F). A similar distribution of xGlu immunoreactivity was observed in columnar NPE cells and cuboidal PE cells of the *pars plana* (posterior obicularis ciliaris). Also, high concentrations of xGlu immunoreactivity were detected at the apical surfaces of many of the columnar NPE cells (Figure 1G, H). In addition, xGlu immunoreactivity was detected in ciliary muscle (Figure 1G, H), corneal endothelial cells, cells of the anterior iris border (limiting) layer, iris thick walled blood vessels (Figure 1I, J), iris stromal melanocytes (Figure 1B, I, J), and pigmented cells/dilator muscle cells of the posterior iris (Figure 1A, B, I, J).

Detection of xGlu immunoreactivity in monkey ciliary body and iris tissue

XGlu immunoreactivity was detected in monkey ciliary body epithelial and iris cells (Figure 2). High concentrations of xGlu immunoreactivity were detected in monkey *pars plicata* ciliary body PE and NPE cells (Figure 2A, B). The intensity of the xGlu signal in monkey PE cells was similar to that in the adjacent NPE cells (Figure 2C, D). However, high concentrations of xGlu immunoreactivity were noted at the apical surface in several NPE cells (Figure 2C, D). XGlu immunoreactivity was also detected in the columnar NPE cells and cuboidal PE cells of the monkey *pars plana* tissue (Figure 2E, F). Also, high concentrations of xGlu immunoreactivity were detected in the monkey anterior iris pigment epithelial/dilator muscle cell layer along the posterior iris surface, in melanocytes within the iris stroma, and in endothelial cells at the anterior surface of the iris (Figure 2G, H). Thus, these results suggest that the distribution of xGlu immunoreactivity is similar in human and monkey anterior uveal tissue.

Detection of GLAST-I and GS in human uveal tissue by Western blot analysis

Based upon the detection of GLAST-1 and GS in retina (Kugler and Beyer 2003), the importance of GS to visual function (Barnett et al 2000) and regulation of Glu and ammonia in the retina (Derouiche and Rauen 1995) as well as the detection of GS in rat retina and ciliary body (Riepe and Norenberg 1978), it was of interest to determine if GLAST-1 and GS were expressed in human iris and ciliary body tissue. GLAST-1 and GS immunoreactive proteins were detected in iris, ciliary body, and retinal tissue lysates by western blot analysis (Figure 3). GLAST-1 (52 kDa) and GS (40 kDa) protein bands were detected in iris, ciliary body, retinal pigment epithelium (RPE), and nerve fiber layer (NFL) lysates. Higher molecular weight isoforms of GS (68, 72 and/or 74 kDa) were detected in retinal tissue lysates (Figure 3B). These results suggest that GLAST-1 and GS proteins are expressed in human iris, ciliary body, and retina tissue.

Co-localization of xGlu immunoreactivity, GLAST-I, and GS

Next, dual IFA analysis was employed to demonstrate the cellular localization of GLAST-1 with xGlu and GS with xGlu in human ciliary body tissue (Figure 4). Polyclonal antibody to a synthetic C-terminal peptide of rat GLAST-1 reacted with corneal endothelial cells, iris melanocytes, iris

pigment epithelial/dilator muscle cells, and ciliary body PE and NPE cells (Figure 4A, B). Moreover, GLAST-1 was detected in the cytoplasm of PE and NPE cells, on the basal surface of PE cells, and on the apical and basal surfaces of NPE cells of the *pars plicata* (Figure 4D). GLAST-1 was also detected in the cytoplasm of cuboidal PE and columnar NPE cells, on the basal surface of the cuboidal PE cells, and on the apical and basal surfaces of the columnar NPE cells of the *pars plana* ciliary body (Figure 4G). GLAST-1 was detected on *pars plicata* and *pars plana* ciliary body NPE cells that contained high concentrations of xGlu immunoreactivity (Figure 4C–H). Antibody to GS reacted with GS protein in the cytoplasm of xGlu positive PE and NPE cells and blood vessels (Figure 4I–K). These results suggest that human ciliary body PE and NPE cells contain xGlu, GLAST-1, and GS.

Serum/AH Gln, Ala, and Glu concentration gradients

The results of the studies above support the idea that GLAST-1 on NPE cell may actively remove Glu from the AH and that the transported Glu could be converted by GS to Gln in the presence of free ammonia as reported for retinal cells (Derouiche et al 1995; Shaked et al 2002). If so, one would predict that the Glu concentration in AH to be lower and the Gln concentration to be higher than in plasma. To assess the serum to AH concentration gradients, the Glu, Gln, and Ala concentrations in paired AH and serum samples from the monkeys and cataract patients were determined (Table 2). The mean Glu concentration (\pm standard deviation) in monkey AH (14 ± 5 nanamoles/ml; $n = 10$; was 3.2-fold lower than in serum (45 ± 14 nanamoles/ml; $n = 5$; $p = 0.005$), while the Glu concentration in cataractous AH (7.5 ± 4.6 nanamoles/ml; $n = 10$) was 9.6 fold-lower than in paired human serum (72 ± 24 nanamoles/ml; $n = 10$; $p < 0.001$). Concomitantly, the AH Gln concentrations was higher than in paired serum from monkeys (587 ± 18 nanamoles/ml versus 392 ± 138

nanamoles/ml; $p = 0.01$; S/AH ratio, 0.67:1) and humans (632 ± 132 nanamoles/ml versus 607 ± 91 nanamoles/ml; $p = 0.15$; S/AH ratio, 0.96:1). No differences were detected between Ala concentrations in paired monkey AH and serum samples (147 ± 27 nanamoles/ml versus 158 ± 39 nanamoles/ml, respectively; S/AH ratio, 0.93:1) or in paired human AH and serum samples (255 ± 93 nanamoles/ml versus 232 ± 34 nanamoles/ml, respectively; S/AH ratio, 0.91:1). The results suggest that the Glu concentration is lower, while the Gln concentration is higher in AH than serum and are consistent with Glu, Gln, and Ala concentrations reported in human and monkey AH (Reddy 1967; Reddy et al 1977; Wu et al 1988; Dreyer et al 1996; Warmesley et al 2005). Taken together, the results support the possibility that the S/AH Glu and Gln gradients in human and monkey eyes may be due in part to uptake of Glu from the AH by ciliary body epithelial cells and release of Gln generated by GS.

Discussion

Immunoreactive xGlu was detected in the metabolically active cells that line the anterior and posterior chambers of human and monkey eyes. Accordingly, high levels of xGlu immunoreactivity were detected in cells lining the posterior cornea, anterior limiting, or border layer of the iris, cell bi-layer at the posterior iris surface, PE and NPE cells lining the *pars placata* and *pars plana* ciliary body. In addition, xGlu immunoreactivity was detected in the branching pigment-bearing melanocytes within the iris stroma, thick-walled iris blood vessels, iris pigment epithelial/dilator muscles, and ciliary muscle cells. Most notably, xGlu immunoreactivity was highly concentrated at the apical surface of ciliary body NPE cells. Interestingly, the distribution of xGlu immunoreactivity in NPE cells appeared to be similar to the distribution of pigment granule in PE cells (ie, a gradient across the cell with the highest concentrations on the apical side). The high concentration of xGlu immunoreactivity at the apical surface of NPE cells is likely fostered by the apical – apical apposition

Table 2 Gln, Ala, and Glu concentrations in serum and AH from normal monkeys and inpatients with a cataractous (CAT) lens

Samples from:	Serum (nanamoles/ml)			AH (nanamoles/ml)		
	Glu	Ala	Gln	Glu	Ala	Gln
Monkey (n=5)S/AH ratio	45 ± 14	147 ± 27	392 ± 138	14 ± 5^p 3.2:1	158 ± 39 0.93:1	587 ± 18^a 0.67:1
Hu CAT (n=10)S/AH ratio	72 ± 24	233 ± 34	607 ± 91	7.5 ± 4.6^b 9.6:1	255 ± 93 0.91:1	632 ± 132 0.96:1

Note: Paired student test; $^p < 0.01$; $^b \leq 0.005$

Abbreviations: AH, aqueous humor; Ala, alanine; Gln, glutamine; Glu, glutamate; S, serum.

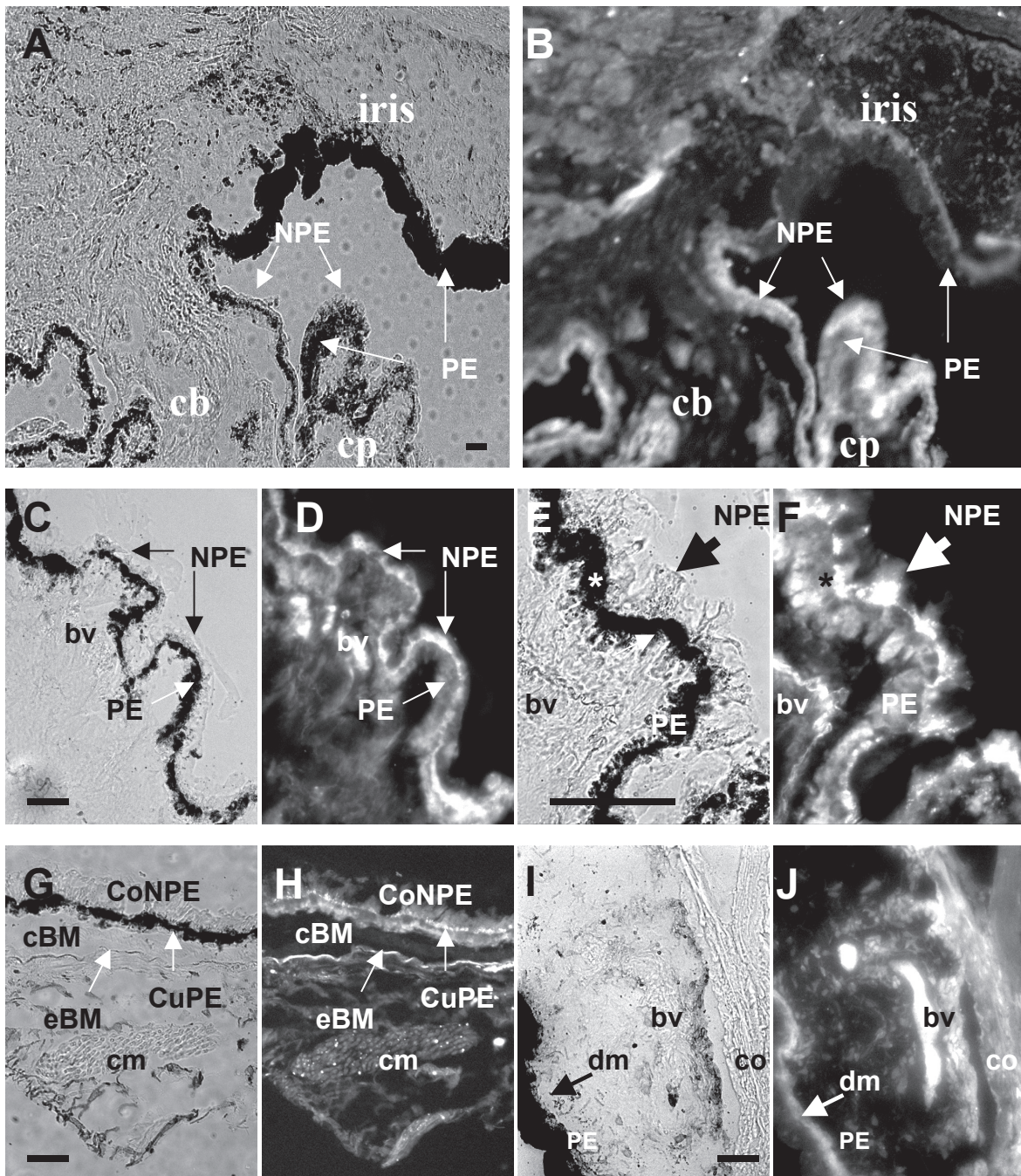


Figure 1 Distribution of xGlu immunoreactivity in anterior uveal tissues from human cadaver eyes. (A) Light photomicrograph of the iris/ciliary body (cb) of the #3 human eye (Table 1) and corresponding (B) IFA photomicrograph showing xGlu immunoreactivity in epithelial cells that line the anterior and posterior iris and ciliary body. Note the intense immunofluorescence staining of the ciliary process (cp) epithelial cells. (C) High magnification light photomicrograph of human ciliary body *pars plicata* tissue from the #2 donor eye and (D) corresponding IFA photomicrograph showing the intense xGlu immunoreactivity signal in NPE cells. (E) Higher magnification light photomicrograph of human ciliary body tissue from the #1 donor eye and (F) the corresponding IFA photomicrograph showing intense xGlu immunoreactivity in PE and NPE cells (*). Note the highly intense immunofluorescent signal at the apical surface of the NPE cells adjacent to the apical surface of the PE cells (large arrow). (G) Light photomicrograph of human *pars plana* tissue from the #3 donor eye and corresponding (H) IFA photomicrograph showing xGlu immunoreactivity in the columnar NPE (CoNPE) and cuboidal PE (CuPE) cells of the *pars plana*. Also, note the high concentration of xGlu immunoreactivity at the apical surface of the CoNPE cells and in ciliary smooth muscle (cm) cells of the #3 donor eye. (I) Light photomicrograph of #2 donor iris and the corresponding (J) IFA photomicrograph showing xGlu immunoreactivity in the cornea (co) cells, iris pigment epithelium and dilator muscle (dm) cell layer; thick walled blood vessels (bv), melanocytes of the vascular layer; and pigment cells on the anterior border of the iris surface. (Bar = 50 μ m).

Abbreviations: bv, blood vessel; cb, ciliary body; cm, ciliary muscle; CoNPE, columnar NPE; cp, ciliary process; CuPE, cuboidal PE; cBM, cuticle layer of Bruch's membrane; dm, dilator muscle; eBM, elastic layer of Bruch's membrane; Gln, glutamine; IFA, immunofluorescent-antibody; NPE, nonpigmented epithelial; PE, pigmented epithelial; xGlu, cross-linked glutamate.

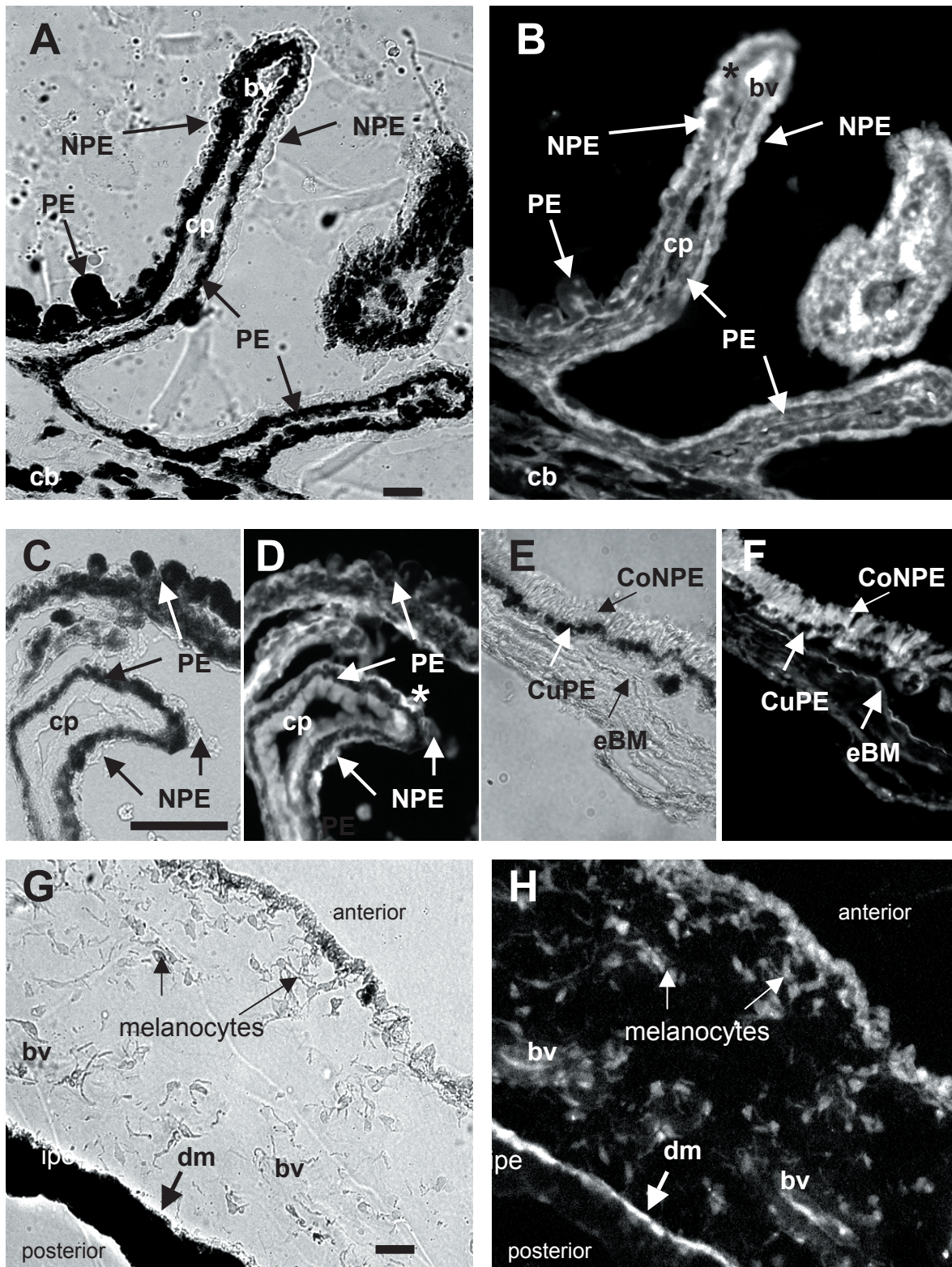


Figure 2 Distribution of xGlu immunoreactivity in monkey ciliary body (cb) and iris tissue. (A) Light photomicrograph and (B) IFA showing xGlu immunoreactivity in the PE and NPE cells of #1 monkey *pars plicata* ciliary processes (cp). Note the higher concentration of xGlu immunoreactivity at the apical surface of some of the NPE cells (*). (C) Light photomicrograph of a high power magnification of a section of #2 monkey ciliary body tissue and (D) the corresponding IFA section showing xGlu immunoreactivity in PE and NPE cells with high concentration of xGlu immunoreactivity at the apices of some NPE cells (*). (E) Light photomicrograph of *pars plana* tissue and (F) the corresponding IFA showing a similar distribution of concentrated xGlu immunoreactivity in cuPE and coNPE cells (anterior to the elastic Bruch's membrane; eBM) as in *para plana* tissue. (G) Light photomicrograph of iris tissue and (H) corresponding IFA showing xGlu immunoreactivity in the anterior iris cells, iris melanocytes, blood vessel (bv) cells, and pigment containing epithelial/dilator muscle (dm) cells. (Bar = 50 mm).

Abbreviations: bv, blood vessel; cb, ciliary body; cm, ciliary muscle; CoNPE, columnar NPE; cp, ciliary process; CuPE, cuboidal PE; eBM, cuticle layer of Bruch's membrane; dm, dilator muscle; eBM, elastic layer of Bruch's membrane; Gln, glutamine; IFA, immunofluorescent-antibody; NPE, nonpigmented epithelial; PE, pigmented epithelial; xGlu, cross-linked glutamate.

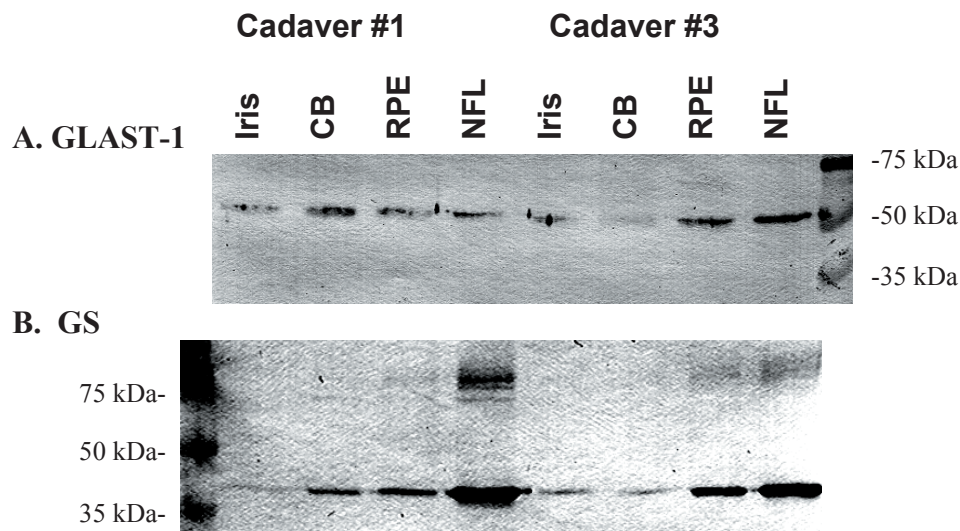


Figure 3 Western blot analysis for (A) GLAST-1 and (B) GS protein expression in iris, ciliary body (CB), retinal pigmented epithelium (RPE) and nerve fiber layer (NFL) tissues from 2 human cadaver eyes (5 µg protein/lane).

Abbreviations: GLAST-1, a glutamate transporter; GS, glutamine synthetase.

of the PE and NPE cells (ie, in most cases amino acids are transported from the apical to basal surface) and could be due to several mechanism(s). That is, the xGlu immunoreactivity pattern in NPE cells could be due in part to Glu uptake by EAATs, Glu exchanger activity (Enkvist and McCarthy 1994; Schultz and Stell 1996), anaerobic glycolysis in ciliary body tissue (deRoethth 1954) or postmortem changes.

The detection of high affinity GLAST-1 on cells that line the anterior chamber lumen (ie, corneal endothelium, iris melanocytes, and iris pigmented cells and ciliary body PE and NPE cells) suggests they may actively take up extracellular Glu as reported for GLAST-1 in brain, retinal, myocardial, and renal cells (Schultz and Stell 1996; Lehre et al 1997; Rauen et al 1998; Welbourne et al 2001; Ralphe et al 2004). Moreover, the high intracellular concentration of xGlu immunoreactivity in NPE cells and the lower than plasma concentration of AH Glu suggest that GLAST-1 on NPE cells may take up Glu from the AH. Notably, GLAST-1 and xGlu immunoreactivity were detected in iris pigment epithelial/dilator muscle, ciliary body blood vessel wall, and ciliary muscle cells. The detection of GLAST-1 and xGlu immunoreactivity in iris and ciliary body muscles is consistent with the reports of GLAST-1 and Glu in myocardium (Ralphe et al 2004) and of Glu in smooth muscle (Quesada et al 1993). Taken together, the results are consistent with the suggestion that GLAST-1 may play a role in maintain the high intracellular levels of Glu in human and monkey iris and ciliary body tissues, but they do not rule out the possibility

that other EAATs may be present in human and monkey iris and ciliary body tissue. The likelihood that other EAAT are present is supported by the reports that different EAATs are associated with different cells within the retina (Schultz and Stell 1996; Arriza et al 1997; Pow et al 2000), all 5 EAAT subtypes are present in rat lens (Lim et al 2005), multiple EAATs may be expressed on a cell (Welbourne et al 2001; Ward et al 2004), EAAT2 has been detected in rabbit ciliary body (Langford et al 1997) and EAAT-3 has been detected in rat ciliary body tissue (Hu et al 2005). Further, the possibility that other Glu transport systems (Sweiry et al 1995; Bridges et al 2001) and alternate metabolic pathways (eg, leucine to Glu) (Schachter and Sang 2002) may also contribute to the high intracellular concentration of xGlu in human iris and ciliary body cells cannot be ruled out.

The detection of GS in PE and NPE cells suggests metabolism of Glu to Gln in ciliary body tissue as in retina and kidney tissue (Riepe and Norenberg 1978; Welbourne et al 2001). Accordingly, Glu transported into the PE and NPE cell may be amidated by GS to form Gln. Moreover, the co-detection of GLAST-1 and GS in NPE cells supports the possibility that GLAST-1 and GS (Derouiche et al 1995; Shaked et al 2002) may play a role in the regulation of Glu, ammonia and Gln within the ciliary body tissue and AH. Thus, the low Glu and high Gln levels in AH observed in this and previously studies (Reddy 1967; 1977; Wu et al 1988) could be due in part by GLAST-1 and GS activity in ciliary body tissue. The importance of GS in ciliary body tissue, is further suggested

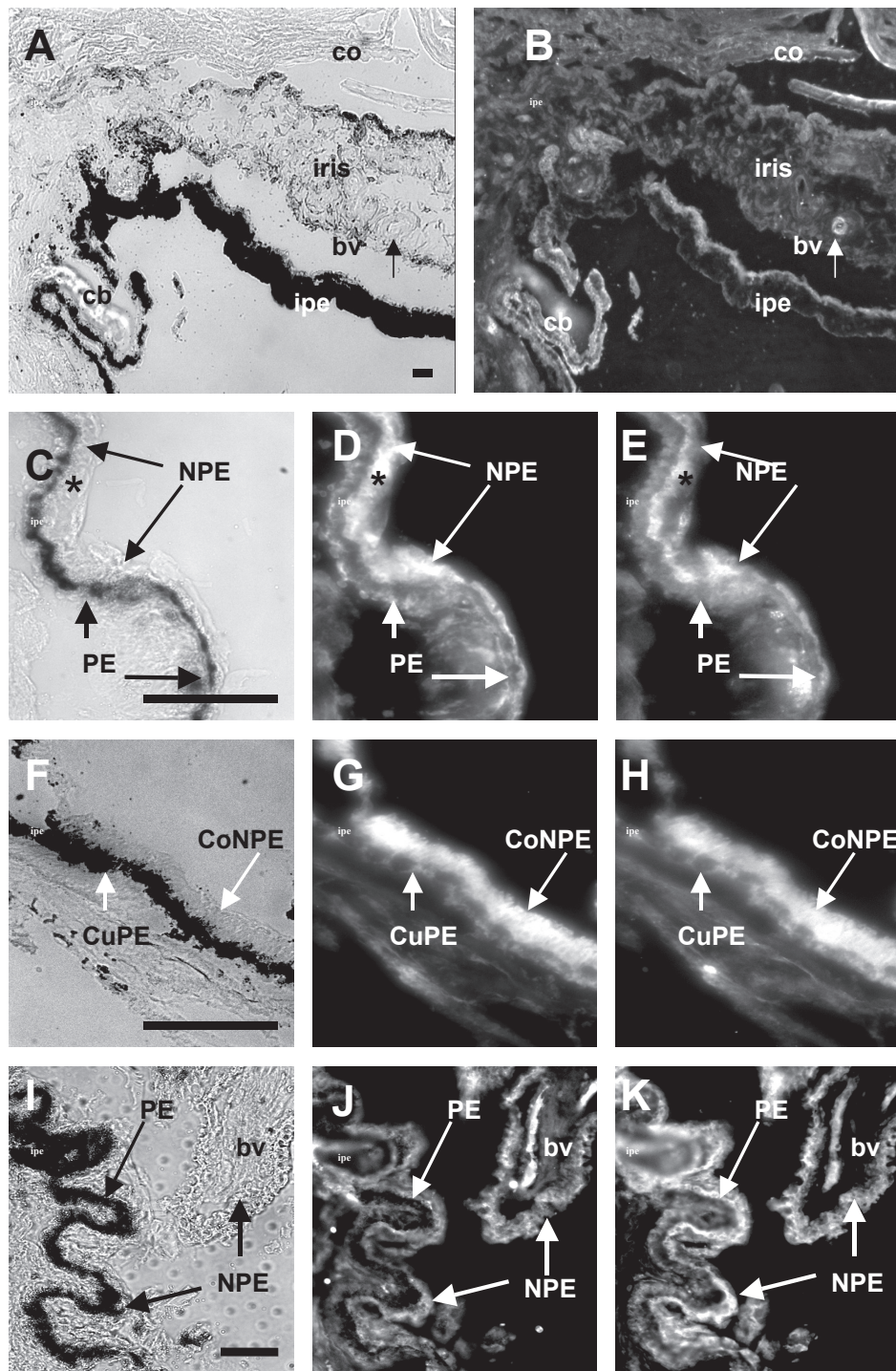


Figure 4 Distribution of GLAST-I and GS with xGlu immunoreactivity in human anterior uveal tissue. (A) Light microscopy of a human iris and ciliary body (cb) tissue section from the #2 cadaver eye. (B) Fluorescent microscopy of the same tissue section showing intense GLAST-I immunoreactivity in cornea endothelium (co), thick walled iris blood vessel (bv), iris pigment epithelium/dilator muscle cells (ipe), and PE and NPE cells that line the ciliary body (cb). (C) High magnification of ciliary body epithelia. (D) High power of the same section showing the distribution of immunoreactive GLAST-I to the basal surface of PE and the basal and apical surfaces of NPE cells. (E) Corresponding high power magnification of the same section showing the distribution of xGlu immunoreactivity in PE and NPE cells with concentrated xGlu immunoreactivity localized to the apical side of NPE cells juxtaposed to the melanosome at the apical side of the PE cells. Note that GLAST-I was detected on the basal PE and apical NPE surfaces and was associated with concentrated xGlu immunoreactivity (*) in NPE cells. (F) High power light microscopy of human *pars plana* ciliary body tissue. (G) Corresponding fluorescent microscopy showing cuboidal PE (cuPE) and columnar NPE (coNPE) cells positive for GLAST-I. (H) Distribution of xGlu immunoreactivity in the same *pars plana* tissue section. (I) High power light microscopy of #3 donor ciliary body tissue with (J) corresponding fluorescent microscopy showing blood vessels, PE and NPE cells positive for GS immunoreactivity. (K) Distribution of xGlu immunoreactivity in the same section. Note that xGlu positive NPE cells were positive for GS (Bar = 50 μ m).

Abbreviations: GLAST-I, a glutamate transporter; GS, glutamate synthetase; IFA, immunofluorescent-antibody; NPE, nonpigmented epithelial; PE, pigmented epithelial; xGlu, cross-linked glutamate.

by studies indicating that Glu is the source of Gln in rat ciliary body tissue (ie, inhibited by methionine sulfoximine) (Hu et al 2005).

The immunohistochemical detection of high levels of xGlu, GLAST-1, and GS ciliary body tissue supports the concept that perturbation of Glu levels or high affinity Glu transport activity can affect BAB permeability via the paracellular pathway between PE and NPE cells (Langford et al 1997; 1999). The role of Glu in the paracellular permeability model (Langford et al 1997) is consistent with the reports that GLAST-1, GS, and/or Glu/Gln levels can modulate cell volume (Izumi et al 2004; Welbourne et al 2001), tight junction proteins (Li et al 2004), gap junction communication between cells (Enkvist and McCarthy 1994) and blood-retina barrier permeability (Frohlich and Klessen 2000). Additional studies are needed to assess the effects of different Glu transporters and GS on Glu levels in ciliary body tissue and on BAB paracellular permeability.

In summary, the distribution of xGlu immunoreactivity in the anterior uveal tissues of human and monkey eyes is similar. Notably, high levels of xGlu immunoreactivity were detected in GLAST-1 and GS positive ciliary body NPE cells. The low Glu and high Gln AH concentrations and the high concentration of Glu in GLAST-1 and GS positive NPE cells support the possibility that GLAST-1 (and other EAATs) and GS play a role in maintaining intracameral Glu gradients. Further, the results provide immunohistochemical support for the idea that pharmaceutical agents and systemic diseases that perturb Glu/Gln concentrations, GLAST-1, and/or GS activities may affect the barrier function of iris and ciliary body tissue.

Acknowledgments

The authors thank Christopher Duggan, Jing Wen Ma, and Kathleen Llorens (Director, Core Research Laboratory, LSUHSC-S) for technical assistance. This work was supported in part by the Clinical Faculty of the Department of Ophthalmology, LSUHSC, Shreveport, LA and an unrestricted grant from Alcon Laboratories (Fort Worth, TX) to the LSUHSC Ophthalmology Resident Education and Research Program.

References

- Arriza JL. 1994. Functional comparisons of three glutamate transporter subtypes cloned from motor cortex. *J Neurosci*, 14:5559–69.
- Arriza JL, Eliasof S, Kavanaugh MP, et al. 1997. Excitatory amino acid transporter 5, a retinal glutamate transporter coupled to a chloride conductance. *Proc Natl Acad Sci U S A*, 94:4155–60.
- Barnett NL, Pow DV, Robinson SR. 2000. Inhibition of Müller cell glutamine synthetase rapidly impairs the retinal response to light. *Glia*, 30:64–73.
- Bridges CC, Kekuda R, Wang H, et al. 2001. Structure, function, and regulation of human cystine/glutamate transporter in retinal pigment epithelial cells. *Invest Ophthalmol Vis Sci*, 42:47–52.
- Choi DW, Maulucci-Gedde M, Kriegstein AR. 1987. Glutamate neurotoxicity in cortical cell culture. *J Neurosci*, 7:357–68.
- Chen D, Texada DE, Duggan C, et al. 2005. Surface calreticulin mediates muramyl dipeptide induced apoptosis in RK₁₃ cells. *J Biol Chem*, 280:22425–36.
- Davanger S, Ottersen OP, Storm-Mathisen J. 1991. Glutamate, GABA and glycine in the human retina: an immunocytochemical investigation. *J Comp Neurol*, 331:483–94.
- Derouiche A, Rauen T. 1995. Coincidence of L-glutamate/L-aspartate transporter (GLAST) and glutamine synthetase (GS) immunoreactions in retinal glia: evidence for coupling of GLAST and GS in transmitter clearance. *J Neurosci Res*, 42:131–43.
- Dreyer EB, Zurakowski D, Schumer RA, et al. 1996. Elevated glutamate levels in the vitreous body of human and monkeys with glaucoma. *Arch Ophthalmol*, 114:299–305.
- Ehinger B. 1977. Glial and neuronal uptake of GABA, glutamic acid, glutamine, glutathione in the rabbit retina. *Exp Eye Res*, 25:221–34.
- Enkvist MO, McCarthy KD. 1994. Astroglial gap junction communication is increased by treatment with either glutamate or high K⁺ concentration. *J Neurochem*, 62:489–95.
- Fonseca-Wollheim F. 1990. Preanalytical increase of ammonia in blood specimens from healthy subjects. *Clin Chem*, 36:1483–7.
- Frohlich E, Klessen C. 2000. Glutamine synthetase and marker enzymes of the blood-retina barrier in fetal bovine retinal pigment epithelial cells. *Graefes Arch Clin Exp Ophthalmol*, 238:500–7.
- Hu R, Donaldson PJ, Kalloniatis M. 2005. Amino acid localization and transport in the ciliary epithelium of the rat eye. *Invest Ophthalmol Vis Sci*, 46:E3322.
- Izumi Y, Matsukawa M, Benz AM, et al. 2004. Role of ammonia in reversal of glutamate-mediated Muller cell swelling in the rat retina. *Glia*, 48:44–50.
- Jernigan Jr HM, Zigler Jr JS. 1987. Metabolism of glutamine and glutamate in monkey lens. *Exp Eye Res*, 44:871–6.
- Jernigan Jr HM. 1990. Metabolism of glutamine and glutamate in human lens. *Exp Eye Res*, 50:597–601.
- Kalloniatis M, Marc RE, Murry RF. 1996. Amino acid signatures in primate retina. *J Neurosci*, 16:6807–29.
- Kanai Y, Stelzner M, Nubberger S, et al. 1994. The neuronal and epithelial human high affinity glutamate transporter. *J Biol Chem*, 269:20599–606.
- Kugler P, Beyer A. 2003. Expression of glutamate transporters in human and rat retina and rat optic nerve. *Histochem Cell Biol*, 120:199–212.
- Langford MP, Berg ME, Mack JA, et al 1997. Inhibition of glutamate uptake causes an acute increase in aqueous humor protein. *Exp Eye Res*, 64:157–65.
- Langford MP, Chen D, Neff AG, et al. 1999. Intracameral muramyl dipeptide-induced paracellular permeability associated with decreased glutamate transporter and γ -glutamyltranspeptidase activities. *Exp Eye Res*, 68:591–600.
- Langford MP, Chen D, Gosslee J, et al. 2006. Intracameral toxicity of bacterial components muramyl dipeptide and staurosporine; ciliary cyst formation, epithelial cell apoptosis and necrosis. *Cutan Ocul Toxicol*, 25:85–101.
- Lehre KP, Davanger S, Danbolt NC. 1997. Localization of the glutamate transporter protein GLAST in rat retina. *Brain Res*, 744:129–37.
- Li N, Lewis P, Samuelson D, et al. 2004. Glutamine regulates Caco-2 cell tight junction proteins. *Am J Physiol Gastrointest Liver Physiol*, 287:G726–G733.
- Lim J, Lam YC, Kistler J, et al. 2005. Molecular characterization of the cystine/glutamate exchanger and the excitatory amino acid transporters in the rat lens. *Invest Ophthalmol Vis Sci*, 46:2869–77.
- Marc RE, Murry RF, Fisher SK, et al. 1998. Amino acid signatures in normal cat retina. *Invest Ophthalmol Vis Sci*, 39:1685–93.

- Marc RE, Cameron D. 2001. A molecular phenotype atlas of the zebrafish retina. *J Neurocytol*, 30:593–654.
- Meade D, Chess C, Welbourne TC. 1998. Glutamate transport and cellular glutamine metabolism: regulation in LLC-PK1 and LLC-PK1-F+ cell lines. *Am J Physiol Cell Physiol*, 274:C1616–C1624.
- Pow DV, Barnett NL, Penfold P. 2000. Are neuronal transporters relevant in retinal glutamate homeostasis? *Neurochem Int*, 37:191–8.
- Quesada O, Lu P, Sturman JA. 1993. Taurine distribution in different cat muscles as visualized by immunohistochemistry: changes with stimulus state. *Cytobios*, 73:143–54.
- Ralphe JC, Segar JL, Schutte BC, et al. 2004. Localization and function of the brain excitatory amino acid transporter type 1 in cardiac mitochondria. *J Mol Cell Cardiol*, 37:33–41.
- Rauen T, Taylor WR, Kuhlbrodt K, et al. 1998. High-affinity glutamate transporters in the rat retina: a major role of the glial glutamate transporter GLAST-1 in transmitter clearance. *Cell Tissue Res*, 291:19–31.
- Reddy DVN. 1967. Distribution of free amino acids and related compounds in ocular fluids, lens, and plasma of various mammalian species. *Invest Ophthalmol*, 6:478–83.
- Reddy VN, Thompson MR, Chakrapani B. 1977. Amino acid transport across blood-aqueous barrier of mammalian species. *Exp Eye Res*, 25:555–62.
- Riepe RE, Norenberg MD. 1978. Glutamine synthetase in the developing rat retina: an immunohistochemical study. *Exp Eye Res*, 27:435–44.
- deRoeth A Jr. 1954. Glycolytic activity of ciliary processes. *AMA Arch Ophthalmol*, 51:599–608.
- Schachter D, Sang JC. 2002. Aortic leucine-to-glutamate pathway: metabolic route and regulation of contractile responses. *Am J Physiol Heart Circ Physiol*, 282:H1135–H1148.
- Schultz K, Stell WK. 1996. Immunocytochemical localization of the high-affinity glutamate transporter EAAC-1, in the retina of representative vertebrate species. *Neurosci Lett*, 211:191–4.
- Shaked I, Ben-Dror I, Vardimon L. 2002. Glutamine synthetase enhances the clearance of extracellular glutamate by neural retina. *J Neurochem*, 83:574–80.
- Shen F, Chen B, Danias J, et al. 2004. Glutamate-induced glutamine synthetase expression in retinal Müller cells after short-term ocular hypertension in the rat. *Invest Ophthalmol Vis Sci* 45:3107–12.
- van Staaten HW, He Y, van Duist MM, et al. 2006. Cellular concentrations of glutamine synthetase in murine organs. *Biochem Cell Biol*, 84:215–31.
- Sweiry JH, Sastre J, Vina J, et al. 1995. A role for γ -glutamyl transpeptidase and the amino acid transport system x_c^- in cystine transport by a human pancreatic duct cell line. *J Physiol* 485:167–77.
- Ward MW, Jobling AI, Puthussery T, et al. 2004. Localization and expression of the glutamate transporter, excitatory amino acid transporter 4, within astrocytes of the rat retina. *Cell Tissue Res*, 315:305–10.
- Wamsley S, Gabelt B'AT, Dahl DB, et al. 2005. Vitreous glutamate concentration and axon loss in monkeys with experimental glaucoma. *Arch Ophthalmol*, 123:64–70.
- Welbourne TC, Chavelier D, Mu X. 1996. Glutamate transport modulation of paracellular permeability across LLC-PK-F+ monolayers. *Am J Physiol*, 271:E889–E895.
- Welbourne T, Routh R, Yudkoff M, et al. 2001. The glutamine/glutamate couplet and cellular function. *News Physiol Sci*, 16:157–60.
- Wuu JA, Wen LY, Chuang TY, et al. 1988. Amino acid concentrations in serum and AH from subjects with extreme myopia or senile cataract. *Clin Chem*, 34:1610–13.

